ACS Catalysis

Research Article

pubs.acs.org/acscatalysis

Formation of a Stable Iminol Intermediate in the Redox Regulation Mechanism of Protein Tyrosine Phosphatase 1B (PTP1B)

Hisham M. Dokainish and James W. Gauld*

Department of Chemistry and Biochemistry, University of Windsor, Windsor, Ontario N9B 3P4, Canada

Supporting Information

ABSTRACT: Protein tyrosine phosphatase 1B (PTP1B) is a key enzyme in a variety of physiological processes including insulin and leptin signaling. Experimentally it has been previously suggested to form an enzyme-derived sulfenyl-amide intermediate as a means of protecting an active site cysteinyl against overoxidation. In this study, key aspects of the mechanism by which PTP1B mediates against overoxidation of its active site cysteinyl has been examined via multiscale computational enzymology (e.g., molecular dynamics simulations and high-level hybrid quantum mechanics/molecular mechanics). Several possible initial reactive complexes containing an active site sulfenic acid (oxidized cysteinyl) were considered, as well as possible reaction pathways and intermediates. Importantly, the only enzymatically feasible mechanism for formation of a putative sulfenyl-amide intermediate occurs via a stepwise pathway. The only feasible mechanism was found to occur in a stepwise fashion, in which a stable iminol intermediate is formed. This step has an activation energy of 48.6 kJ mol^{-1}. Later, a much more stable iminol intermediate is formed in which a noncovalent electrostatic interaction of the sulfenic acid sulfur antibonding orbital with the iminol nitrogen lone pair was found to occur. Subsequently, a cyclic sulfenyl-amide is formed with a concomitant proton transfer from Glu115 to the sulfenic acid oxygen. Our results suggest that Glu115 and His214 play a crucial role in the mechanism. These results could contribute to the discovery of PTP1B inhibitors and the stabilization of the enzyme oxidized form.

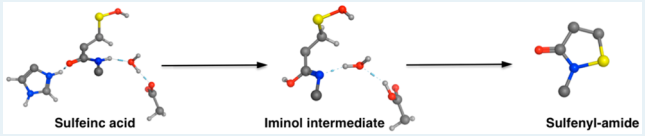

KEYWORDS: *enzyme catalysis, quantum mechanic/molecular mechanics (QM/MM), molecular dynamics (MD) simulations, sulfenic acid, sulfenyl-amide, amide−iminol tutomerization, S···N noncovalent interaction*

INTRODUCTION

Protein tyrosine phosphatases (PTP's) are a large family of enzymes responsible for dephosphorylating phosphorylated tyrosyl residues in proteins,[1,2] a physiologically important post-translational modification (PTM). In particular, the subclass PTP1B, first characterized in 1988,[1,3,4] plays a key role in inhibiting insulin and leptin signaling.[5−7] Conversely, it has been shown to have a crucial positive role in signaling of, for instance, cSrc tyrosine kinases in breast cancer[3,8,9] and the ubiquitous Ras proteins.[10] Consequently, PTP1B is considered to be an outstanding drug target for the treatment of several diseases including diabetes, obesity, and cancer.[3,11−13]

PTP1B catalyzes the dephosphorylation of phosphotyrosine via a two-step ping-pong mechanism (Scheme 1).[14] In the first step, the sulfur of an active site cysteinyl (Cys215) nucleophilically attacks the phosphotyrosine ester to form a phosphoenzyme intermediate. This is accompanied by the concomitant release of the tyrosine. In the second step, hydrolysis of the phosphoenzyme intermediate occurs via nucleophilic attack of H_2O upon activation by Asp181. Tiago et al.[14] have previously investigated both steps using X-ray crystallography to characterize transition state analogues.

To date, four different processes have been identified by which the function of PTP1B can be regulated: phosphorylation, sumoylation, proteolysis, and oxidation.[3] In particular, in the latter, Cys215 has been experimentally observed to be reversibly oxidized to a sulfenic acid (Cys251SOH) by reactive oxygen species (ROS).[15] This modification is in part facilitated by the unusually low pK_a (4.5−5.5) for the thiol of Cys215.[1] This oxidative PTM mediates several signaling pathways. For instance, with regards to insulin, the stimulation of transmembrane receptor kinase (RTK) leads to the activation of NADPH oxidase, producing ROS that oxidize Cys215 in PTP1B, thus transiently inhibiting its function.[1] The activity of PTP1B is restored upon reduction by an external thiol such as thioredoxin (Trx), dithiothreitol (DTT), or glutathione (GSH).[16]

In general, sulfenic acid is susceptible to further and irreversible oxidation to sulfinic or sulfonic acid. X-ray crystallographic analysis as well as pulse-chase labeling and mass spectrometry experiments suggested that the sulfenic acid can undergo an intramolecular reaction to give a seemingly unique cyclic sulfenyl-amide species, thus protecting it from further oxidation.[15,17−19] To-date this mechanism has only been observed for PTP1B. But it should be noted that it has been suggested that such an intermediate may occur in other proteins including PTP1α and other protein families such as organic hydroperoxide resistance regulator (OhrR) in *Bacillus*

Received: October 31, 2014
Revised: February 24, 2015
Published: February 26, 2015

© 2015 American Chemical Society

DOI: 10.1021/cs501707h
ACS Catal. 2015, 5, 2195−2202

Scheme 1. Proposed[14,17] Dephosphorylation Mechanism of Phosphotyrosine in PTP1B as well as the Oxidative Regulation Mechanism in PTP1B via Formation of Sulfenyl-Amide and the Subsequent Reactivation

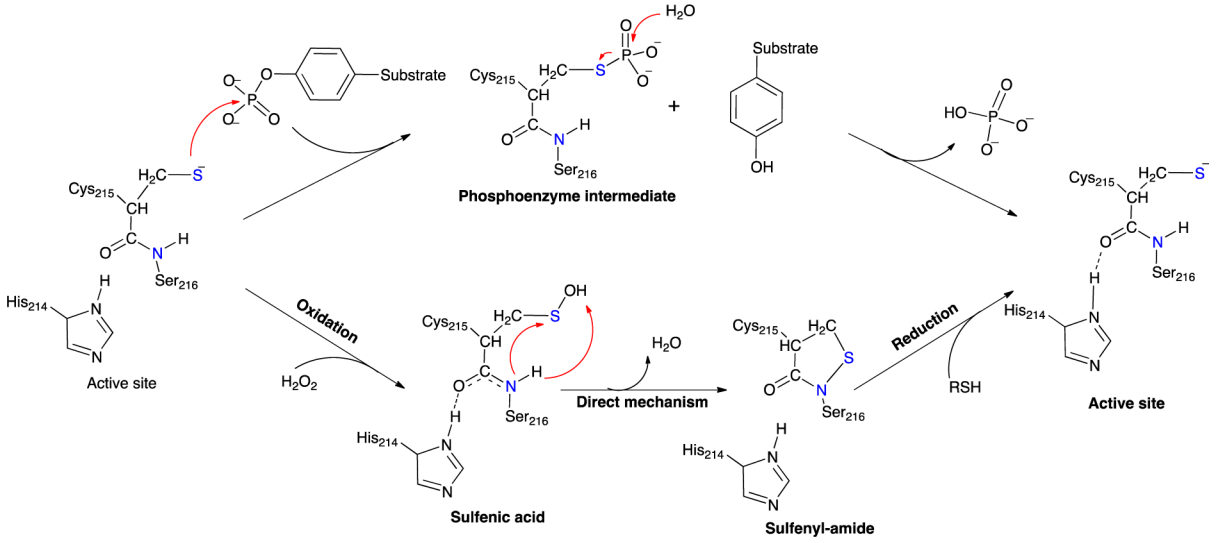

subtilis.[20,21] In other enzymes, sulfenic acid is protected via, for example, formation of a disulfide (e.g., methionine sulfoxide reductase) or hypervalent sulfurane species (e.g., archaeal peroxiredoxin).[22,23]

Initially it was proposed that the sulfenyl-amide forms via a direct S_N2 mechanism. Specifically, the backbone nitrogen of the neighboring serinyl (Ser216) nucleophilically attacks the sulfenic acid's Sγ atom with concomitant release of H_2O (Scheme 1).[17] Furthermore, the hydrogen bonding interaction between the Nδ1 atom of the invariant histidyl (His214) and the carbonyl oxygen of Cys215 was suggested to play a key role in enhancing the nucleophilicity of the Ser216 backbone nitrogen.[17] It is also noted that mutation of His214 to Asn or Ala was shown to increase the pK_a of Cys215.[24] Generation of the sulfenyl-amide intermediate induces an active site conformational change. In particular, formation of the S−N bond disrupts a hydrogen bond between the R-groups of Ser216 and Tyr46, rendering the enzyme inactive.[25] Thus, there is interest in inducing or stabilizing this inactive oxidized form as a potential therapeutic approach for several diseases.[25] It is noted that under experimental conditions, several external thiols have been shown to be able to reduce the sulfenyl-amide, regenerating the activity of the catalytic Cys215.[16] This restoration mechanism has been confirmed via resoaking crystals of sulfenyl-amide with dithiothreitol (DTT).[17]

Sarma et al.[26] have previously studied, both experimentally and computationally, the mechanism of sulfenyl-amide formation in PTP1B using model nonprotein molecules. In particular, formation of sulfenyl-amide via the above proposed direct mechanism was calculated at the B3LYP/6-31G(d) level of theory to have a barrier of 206.2 kJ mol^{-1}. In addition, they considered an alternate mechanism involving heterocyclic substitution of an oxazoline *ortho* to the sulfenic acid moiety. This modification significantly reduced the calculated barrier to 119.8 kJ mol^{-1}. However, they noted that the sulfenic acid model used did "not effectively mimic the cyclization of protein sulfenic acids".[26] Similarly, Sarma et al.[27] examined ortho substitution effects on a small amido thiophenol molecule and concluded that S···N/O interactions could influence the properties of the sulfenic acid. Furthermore, nearby residues may have a role in the sulfenyl-amide formation. More recently, as part of a review, Defelipe et al.[28] discussed results they had obtained for the mechanism of PTP1B using QM/MM. The reactive (QM) region of their chemical model consisted of Cys215 and Ser216. Similar to the results of Sarma et al.,[26] they concluded that the direct formation of sulfenyl amide occurs with a high barrier of 205.0 kJ mol^{-1}. Experimentally, however, several studies have suggested that the rate-limiting step in sulfenyl-amide formation is generation of the sulfenic acid, not the sulfenyl-amide.[15,20] Hence, many questions remain about the enzymatic mechanism.

In this present study, formation of the putative sulfenyl-amide intermediate from a Cys215 derived sulfenic acid, within the enzyme environment, is investigated via complementary application of molecular dynamics simulations and extensive quantum mechanical/molecular mechanical (QM/MM) modeling.

COMPUTATIONAL METHODS

Protein Model Preparation and Molecular Dynamics Simulations. The X-ray crystal structure preparation and the MD analysis were performed using the Molecular Operating Environment (MOE) software package.[29] Molecular dynamics simulations were conducted using the NAMD Molecular Dynamics software.[30] The X-ray crystal structure of the *Homo sapiens* PTP1B in its sulfenic acid oxidation state was used as starting structure and obtained from the PDB structure 1OET.[17]

MOE was used to prepare the protein structure by, for instance, correcting for missing hydrogen atoms. The ionization state of appropriate groups was determined using the protonate 3D application in MOE that assigns each residue's ionization state by minimizing the total free energy of the system, and missing protons were automatically added as determined (e.g., of the eight histidyl residues, only His214 was predicted to be, and thus modeled as, protonated).[31] The structure was spherically solvated once up to 15 Å beyond every protein atom and then minimized using the Amber12:EHT force field. The latter uses Amber 12 parameters for the protein and extended Hückel Theory for parametrizing small molecules.[32−34] In order to allow for thermal relaxation, the

DOI: 10.1021/cs501707h
ACS Catal. 2015, 5, 2195−2202

minimized structure was used as a starting point for a 3 ns MD simulation.

In the MD simulation, all atoms were free to move, and a time step of 2 fs was used. Coulombic interactions were calculated with the PME method, whereas short-range van der Waals interactions were truncated at 8−10 Å. The system was annealed, at a constant volume, from 150 to 300 K over 25 ps, equilibrated at 300 K for 25 ps, heated further to 400 K over 25 ps and then equilibrated for 350 ps. The system was then cooled over 25 ps to 300 K and equilibrated for a further 100 ps. This was followed by a production run in the NPT ensemble at 300 K and 1 bar for 2500 ps.

A cluster analysis using MOE software was performed based on the root-mean-square deviation (rmsd) of the active site residues on the generated structures to give five cluster groups. The average structure of the highest populated group was selected and further minimized using the Amber12:EHT force field. The resulting structure was used for quantum mechanical/molecular mechanical (QM/MM) calculations (see below). The rmsd for several active site interactions were calculated to confirm the consistency of these interactions during the simulation.

QM/MM Models and Calculations. All calculations were performed within the ONIOM scheme as in the Gaussian 09 suite of programs.[35] The QM/MM starting structures were acquired from the above MD preparation using the whole protein. The QM (high) and MM (low) layers were described using the hybrid-meta-exchange-correlation functional M06-2X[36] and Amber96 force field, as implemented in Gaussian 09, respectively.[30] Optimized geometries were obtained using the 6-31G(d,p) basis set for the high layer. All atoms in the systems, including solvent, were free to move. Relative energies were obtained by performing single-point energy calculations on the above optimized structures at the ONIOM(M06-2X/6-311+G(2df,p):Amber96) level of theory. The choice of functional and basis sets was based on a structural benchmarking study of several biological sulfur species in which M06-2X/6-31G(d,p) was concluded to give reasonable agreement with those obtained using QCISD and MP2.[37] Due to the models size and computational cost, frequencies were calculated at the M06-2X/6-31G(d,p) level for only the QM-layer's optimized structure to ascertain the nature of reaction stationary points.[38,39] Topological analysis of the electron densities as well as natural bond orbital (NBO) analysis for certain intermediates were performed at the M062-X/6-311+G(2df,p) level of theory. Topological analysis were performed using the AIM2000 program.[40]

Two chemical models were considered, differing only in the protonation state of His214 in the QM-layer. In model I (Figure 1), the QM layer consisted of the catalytic Cys215 in its sulfenic acid form, Ser216, protonated His214, Ala217, Gly218, Ile219, Gly220, Arg221, Ser222, and Asn111. The charge of the QM region and QM/MM model was +1. Addition of the R group of Glu115, the backbone of Met109 and Leu110, and four active site water molecules were included. In model II, His214 was unprotonated so as to further elucidate its role in sulfenyl-amide formation.

Computational chemistry, and in particular multiscale approaches such as used herein, have established themselves as insightful tools for simulating and studying enzymatic mechanisms, their thermodynamics, and for elucidating the nature of intermediates and transition states (TS).[41−44]

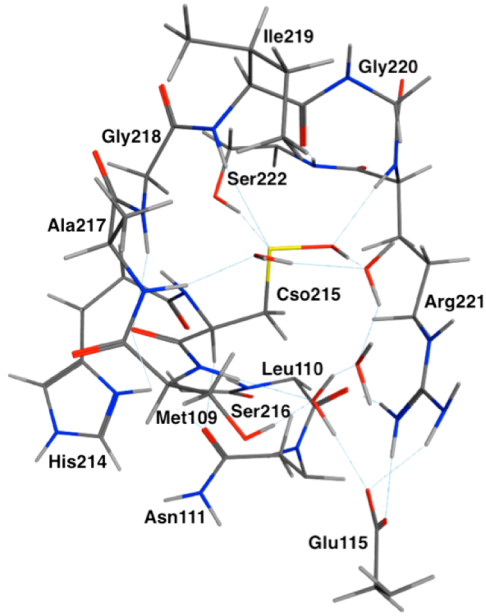

Figure 1. Illustration of the high-layer, QM-region, of the QM/MM model used in this present study (see Computational Methods).

RESULTS AND DISCUSSION

Insights into the Reactive Complex. The previously proposed mechanism suggested an important catalytic role of a hydrogen bond between the imidazole of His214 and carbonyl oxygen of Cys215.[17] Indeed, mutating His214 to Asn or Ala increased the pK_a of Cys216.[24] In a plot of the His214H$^+$···OCys215 distance over the course of the MD simulation (Figure 2), such an interaction is seen to be reasonably

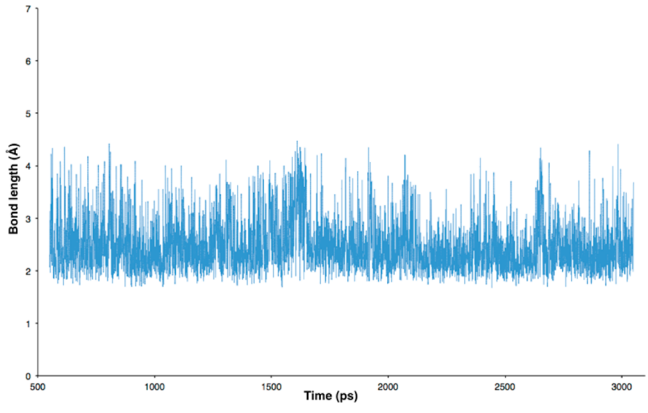

Figure 2. Plot of the His214H$^+$···OCys215 distance (Angstrom) with respect to time (ps) in the MD simulation.

consistent and generally fluctuates between 2 and 3 Å, transiently increasing to 3−4 Å at times, with an average distance over the period of the simulation of 2.61 Å.

At the current QM/MM level of theory (see Computational Methods), two conformers of the reactive complex were obtained, within model 1, that lie just 1.8 kJ mol^{-1} apart in energy; **RC′** and **RC** (the former lying higher in energy). These complexes share a number of important similarities, but they also exhibit key differences (Figure 3).

In particular, in both conformers, the backbone amide nitrogen of Ser216 forms a strong water bridged hydrogen bond network to the side chain carboxylate of Glu115. In the

DOI: 10.1021/cs501707h
ACS Catal. 2015, 5, 2195−2202

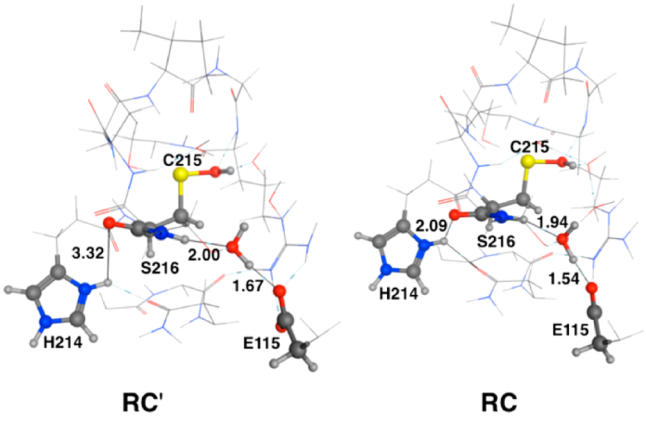

Figure 3. Optimized structures of RC′ and RC obtained for Model I. For clarity, only the QM-layers are shown with the highlighted residues being those involved in the reaction.

higher energy reactive complex (**RC′**), the Ser216-NH···OH_2 distance is 2.00 Å, and the Glu115-COO···OH_2 distance is 1.67 Å. In addition, the protonated guanidinium of Arg221 is also hydrogen bonded to the carboxylate of Glu115, one via each of its terminal $-NH_2$ groups. In **RC**, however, the Ser216-NH···OH_2 and Glu115-COO···OH_2 distances have decreased markedly to 1.94 and 1.54 Å, respectively. Meanwhile, the protonated guanidinium of Arg221 now forms a single hydrogen bond with the carboxylate of Glu115 with a distance of 1.68 Å.

More importantly, however, significant differences are observed in the positioning and interactions of the $His214H^+$ group. Specifically, in **RC′**, it forms a strong hydrogen bond interaction with the side chain carbonyl oxygen of Asn111 with $r(His214H^+\cdots 5OAsn111)$ = 1.93 Å. As a result, $His214H^+$ forms only a weak interaction with the amide oxygen of Cys215; $r(His214H^+\cdots OCys215)$ = 3.32 Å. In contrast, in **RC**, the $His214H^+$ now forms a much weaker interaction with Asn111, $r(His214H^+\cdots OAsn111)$ = 2.10 Å. Instead, it forms a strong hydrogen bond with the carbonyl oxygen of Cys215 with a length of just 2.09 Å (Figure 3).

In both conformers, however, the distance between the sulfenic acid sulfur and the amide nitrogen of Ser216, between which a bond is to be formed, is quite large at 3.83 and 3.74 Å in **RC′** and **RC**, respectively. The following mechanistic studies have begun from **RC** unless otherwise noted.

Direct Formation of a Sulfenyl-Amide. As noted in the introduction Sarma et al.[26] and Defelipe et al.[28] have previously studied the formation of the sulfenyl-amide via a direct mechanism and in both cases found it to have an unfeasibly high barrier of more than 200 kJ mol^{-1}. In the study of Defelipe et al. the optimized structure of the transition state (TS) of the mechanism has large distances of 3.30 and 2.36 Å for the S···N and S···O interactions, respectively.[28] We examined an alternate direct mechanism within the current enzyme models. In particular, in both the MD simulations and QM/MM optimized structures, a water molecule is seen to be positioned near the sulfenic acid and Ser216 amide and may be able to facilitate a direct reaction between these two moieties (Figure S1). However, no such water-facilitated direct reaction could be identified.

The challenges facing a direct mechanism may be partly due to the poor nucleophilicity of the Ser216 nitrogen as a result of being engaged in π-conjugation with the amide bond carbonyl group. However, as detailed above, within the MD structures, as well as the QM/MM optimized structures of both **RC** and **RC′**, it is observed that a water molecule consistently bridges the Ser216-NH backbone group and the side chain carboxylate of Glu115. Thus, we examined possible mechanisms by which Glu115 may facilitate formation of a sulfenyl-amide.

Stepwise Formation of a Sulfenyl-Amide. The potential energy surface (PES) for the mechanism obtained in which Glu115 facilitates the reaction is shown in Figure 4. The optimized structures, with selected bond distances, of the associated stationary points along the mechanism are given in Figure 5.

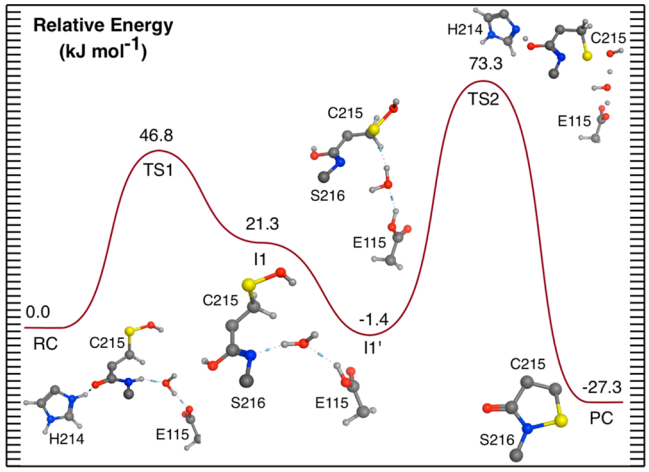

Figure 4. Potential energy surface obtained for the formation of sulfenyl-amide from sulfenic acid via iminol intermediate, see Computational Methods.

Glu115 is able to partake in the mechanism by helping to activate the water that bridges between its carboxylate and the amide NH moiety of Ser216. This step proceeds via the transition structure **TS1** at a cost of only 46.8 kJ mol^{-1}. There are in fact three proton transfers involved in this step as can be seen in the optimized structure of TS1. Although these occur concomitantly, some occur earlier or later than the others. In particular, in **TS1**, the bridging water (H_2O_W) has essentially transferred a proton onto the carboxylate of Glu115 as indicated by $HO_W\cdots HOOC_{Glu115}$ and $_{Glu115}COO^-\cdots H$ distances of 1.67 and 1.01 Å, respectively (Table S1). It is noted that as a result, the extent of hydrogen bonding between Glu115 and Arg221 is reduced. Simultaneously, the length of the cleaving Ser216N···H bond and forming $_{Ser216}NH\cdots O_W$ bonds is 1.27 and 1.23 Å, respectively (Figure 5). The third proton transfer occurs between the protonated imidazole of His214 and the carbonyl oxygen of Cys215, as indicated by $His214\cdots HO_{Cys215}$ and $_{His214}H\cdots O_{Cys215}$ distances of 1.11 and 1.45 Å, respectively (Table S1).

Consequently, in the optimized structure of the subsequent intermediate **I1**, complete proton transfer from His214 to Cys215 carbonyl oxygen has occurred, shifting the double bond from C═O to between the amide nitrogen and carbonyl carbon (C_{Carb}) to give an iminol-type intermediate, whereas Glu115 is now neutral. A similar amide-iminol tautomerization has been recently proposed using model structure of C-terminal aspartic acid residue via two water molecules.[45,46] Energetically, **I1** lies only moderately higher in energy than the initial substrate-bound active site complex **RC** by 21.3 kJ mol^{-1}.

DOI: 10.1021/cs501707h
ACS Catal. 2015, 5, 2195−2202

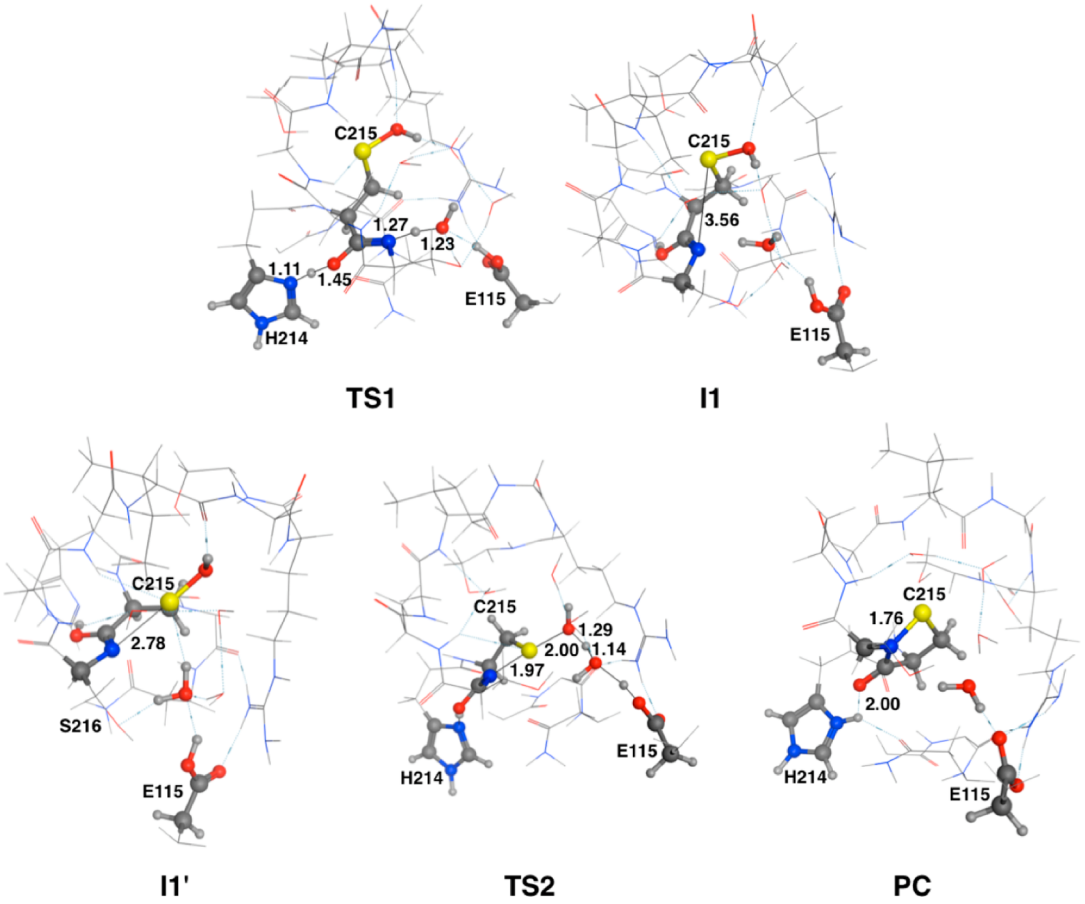

Figure 5. Stationary points obtained for model I for the sulfenyl-amide formation mechanism from sulfenic acid. All atoms in the high QM layer are included in the representation. However, only the highlighted residues are the ones involved in the reaction.

It should be noted that this same step was examined in which the reaction occurs directly from **RC′**. However, no analogous stable **I1** intermediate could be obtained. This likely reflects the fact that **RC′** contains only a very weak hydrogen-bond interaction between His216 and Cys215.

The nucleophilicity of the nitrogen in the iminol isomer is expected to be higher than in the amide isomer and, as such, might facilitate its nucleophilic attack on the sulfenic acid sulfur and the subsequent formation of sulfenyl-amide intermediate. However, the distance between the $_{Cys215}$S and N_{Ser216} in **I1** is quite large, at 3.00 Å. This suggests the need for structural rearrangements in the active site prior to subsequent reactions. An alternate conformer of the iminol intermediate, hereafter referred to as **I1′**, can be obtained via rotation about the $C_{Carb}C_{\alpha}$—CS bond in Cys215 of approximately 31°; specifically, increasing the dihedral angle $\angle C_{Carb}C_{\alpha}CS$ from 99.6° (**I1**) to 130.2° (**I1′**). As a result of this rotation, the distance between the sulfenic sulfur of Cys215 and the nitrogen of Ser216, $_{Cys215}S\cdots N_{Ser216}$, has decreased markedly by 0.22 Å to 2.78 Å. However, at the level of theory used to optimize geometries, an exact value for this rotation was not obtained, and it is expected to be quite small given the relatively modest structural changes observed. For example, upon rotation, the water still forms a hydrogen bond bridge between the Ser216N and Glu115COOH moieties, though now its orientation has changed slightly. In particular, it is now notably closer to the sulfenic acid groups oxygen with $r(O_W\cdots(H)OS_{Cys215})$ = 3.52 Å. In addition, the alternate iminol conformer **I1′** lies 22.7 kJ mol^{-1} lower in energy than **I1**, and in fact is now lower in energy than **RC** by 1.4 kJ mol^{-1} (Figure 4).

The possible occurrence of nonbonded interactions involving protein−sulfur species have recently been gaining attention as they have been suggested to play crucial roles in sulfenic acid chemistry.[47] The existence and nature of any such $_{Cys215}S\cdots N_{Ser216}$ interactions in **I1** and **I1′** were investigated using Quantum Theory Atoms-in-Molecules (QTAIM).[40] In this theory, the presence of a critical point between two atoms can give insights into the nature of the interaction between them.[48] In the case of **I1** no interaction between $_{Cys215}S$ and N_{Ser216} was observed. However, in **I1′**, a critical point between these two centers is observed with an electron density (ρ) of 0.016 and a Laplacian ($\nabla\rho^2$) of 0.017, indicating that these two centers do weakly interact.

Nonbonded electrostatic interaction between S and N centers have been previously reported.[49,50] Such interactions have been suggested to occur via the shift of electron density from the lone pair of the nitrogen to an S−O antibonding orbital (σ^*). Indeed, an NBO analysis on **I1** and **I1′** indicates a slight decrease in the positive charge on the sulfur atom from +0.52 to +0.48 on going from **I1** to **I1′**. In addition, the optimized S−O bond length increases by 0.02 Å to 1.69 Å upon going from **I1** to **I1′** (Table S1). An increase in the electron density on the sulfenic acid oxygen from −0.93 to −0.94 is also observed. Simultaneously, the electron density on the N atom decreases from −0.68 (**I1**) to −0.66 (**I1′**). These values suggest that some charge transfer between $_{Cys215}S$ and N_{Ser216} may occur in **I1′**. It is likely that this noncovalent S···N interaction along

DOI: 10.1021/cs501707h
ACS Catal. 2015, 5, 2195−2202

with the changes in the hydrogen bonding network contribute to the lower relative energy of **I1′** relative to **I1**.

The next and final step of the mechanism is formation of a sulfenyl-amide species. This occurs via **TS2** at a cost of 74.7 kJ mol^{-1} relative to **I1′**, 73.3 kJ mol^{-1} relative to **RC** (Figure 4). In **TS2** the $_{Cys215}S\cdots N_{Ser216}$ distance has decreased by 0.81 Å to 1.97 Å. In addition, however, the proton of the side chain carboxylic acid of Glu115 is transferring to the water (H_2O_W) which is simultaneously transferring a proton onto the sulfenic acid oxygen of Cys215. The latter is illustrated by $O_WH\cdots(H)OS_{Cys215}$ and $HO_{W\cdots}H$ distances of 1.29 and 1.14 Å, respectively (see Figure 5). These proton transfers induce a significant lengthening in the sulfenic acids S−OH from 1.70 Å in **I1′** to 2.00 Å. This step also represents the overall rate-limiting step in the mechanism and is significantly lower than that previously calculated for a direct formation mechanism.[26,28]

The subsequent sulfenyl-amide species (**PC**) formed lies −27.6 kJ mol^{-1} lower in energy than **RC** (Figure 4). As can be seen in Figure 5, a covalent intramolecular $_{Cys215}S-N_{Ser216}$ bond has now been formed with a length of 1.76 Å. Notably, this calculated value is in good agreement with the experimentally measured distance of 1.64 Å obtained for this bond from the X-ray crystal structure PDB ID: 1OES.[17] In **PC**, the imidazole of His214 has also regained the proton it initially transferred in **TS1** onto the Cys215 amide carbonyl oxygen, reforming protonated His214.

As mentioned in the introduction, experimental studies in which the invariant residue His214 was mutated caused an increase in the pK_a of the catalytic Cys215 residue.[24] This was taken to suggest that the imidazole of His214 is protonated in the active site. For completeness, however, we also examined possible mechanisms by which a sulfenyl-amide could be formed in which His214 is initially neutral. No stable intermediate could be obtained analogous to **I1** or **I1′**, but now with an unprotonated Cys215 backbone carbonyl oxygen. This perhaps further underscores the importance of a protonated His214 residue to sulfenyl-amide formation.

We also considered the possibility that a neutral His214 imidazole donates its proton to the Cys215 carbonyl oxygen and abstracts a proton from a nearby residue or network of residues (e.g., Tyr124, His173 and Arg156). That is, the His214 essentially acts as a means to transfer a proton onto the carbonyl oxygen from another nearby residue. However, this possibility was discounted as the proton affinity of the Cys215 carbonyl oxygen is not high enough to be able to abstract a proton from a neutral imidazole and furthermore, no stable analogous **I1** or **I1′** intermediate was obtained. This also suggests that experimental mutation of, for example, His214 to an Asn—i.e., maintain the hydrogen bond interaction with the backbone of Cys215 but without the associated protonated charge—might also inhibit sulfenyl-amide formation.

CONCLUSION

In this present study, several computational methods have been complementarily applied to gain a multiscale understanding of the formation of the physiologically important sulfenyl-amide in the protein trysoine phosphatase PTP1B. More specifically, molecular dynamics (MD), quantum mechanical/molecular mechanical (ONIOM), quantum theory of atoms-in molecules (QTAIM), and natural bond orbital (NBO) analyses have been cooperatively employed. In addition to the overall mechanism, the role of hydrogen bonding and active site waters has also been considered.

Two possible conformers of the substrate-bound active site complex were obtained via MD simulations followed by ONIOM(QM/MM) optimizations. Notably, these complexes, **RC′** and **RC**, primarily differ only in the occurrence of a hydrogen bond between the protonated imidazole of His214 and the backbone amide bond carbonyl oxygen of Cys215 in **RC**. Furthermore, **RC** lies just 1.8 kJ mol^{-1} lower in energy than **RC′**.

An enzymatically feasible water-assisted direct formation mechanism, involving attack of the Cys215-SOH sulfur at the backbone amide N of Ser216, could not be identified.

Starting from **RC**, however, an iminol-type intermediate (**I1**) can be formed via protonation of the carbonyl oxygen of Cys215 by His214. This proceeds with a concomitant proton transfer from the backbone amide N−H of Ser216, via an active site water, onto the carboxyl side chain of Glu115. This step occurs with a barrier of only 46.8 kJ mol^{-1}. Notably, no stable iminol intermediate is obtained without a hydrogen bond between the imidazole of His214 and backbone carbonyl oxygen of Cys215 (i.e., for formation of an iminol *directly* from **RC′**).

Remarkably, the lowest energy conformer of the iminol-type intermediate, **I1′**, lies slightly *lower* in energy than **RC** by 1.4 kJ mol^{-1}, and with a $_{Cys215}S\cdots N_{Ser216}$ distance of 2.78 Å. QTAIM and NBO analysis of **I1′**indicates the presence of a weak interaction between the sulfur of Cys215 and the backbone nitrogen of Ser216. Furthermore, some small charge transfer may occur between the lone pair on $_{Ser216}N$ lone pair and the S−O σ^* orbital.

The final sulfenyl-amide product complex can then be formed in one step via nucleophilic attack of the Cys215 sulfur at the Ser216 backbone nitrogen. This occurs with concomitant transfer of the proton from the previously neutralized carboxylic acid group of Glu115 onto the active site water, which simultaneously transfers a proton onto the hydroxyl oxygen of the sulfenic acid moiety (i.e., Cys215-SOH). This step proceeds with a barrier of 73.3 kJ mol^{-1} with respect to the initial reactant complex RC, or 74.7 kJ mol^{-1} with respect to I1′. It is also the rate-limiting step of the overall reaction. The low barrier for this reaction is due in part to the enhanced nucleophilicity of the nitrogen within the iminol group, relative to when in an amide bond environment, and an increasing contribution from the nitrogen into the σ^* orbital on the Cys215-S−OH bond.

This study also suggests new and expanded roles for Glu115 and His214 in PTP1B, beyond simply as hydrogen bond donors and acceptors. Specifically, they play important roles as mechanistic acid/bases and in stabilizing the iminol tautomer. Indeed, amide−iminol tutomerization is energetically quite feasible, and the iminol tautomer potentially thermodynamically favored or at least on par with the amide tautomer, within an appropriate environment.

ASSOCIATED CONTENT

Supporting Information

The following file is available free of charge on the ACS Publications website at DOI: 10.1021/cs501707h.

Cartesian coordinates and energies of the optimized structures reported herein and figures of the QM/MM

DOI: 10.1021/cs501707h
ACS Catal. 2015, 5, 2195−2202

(expanded QM-region) optimized reactant complex structures (PDF)

AUTHOR INFORMATION

Corresponding Author

*E-mail: gauld@uwindsor.ca. Tel.: (519) 253-3000, ext.3992. Fax: (519) 973-7098.

Notes

The authors declare no competing financial interest.

ACKNOWLEDGMENTS

This work was supported by grants from the Natural Sciences and Engineering Research Council of Canada (NSERC) and the University of Windsor. We acknowledge the Natural Sciences and Engineering Research Council of Canada (NSERC) and University of Windsor for funding, as well as Compute Calcul Canada and SHARCNET for additional computational resources, and we thank Daniel Simard and Bogdan F. Ion for assistance in preparing the manuscript.

ABBREVIATIONS

PTP1B, protein tyrosine phosphatase 1B; PTP, protein tyrosine phosphatases; PTM, post-translational modification; RTK, receptor tyrosine kinase; thioredoxin, Trx; ditiothreitol. DTT; glutathione, GSH; organic hydroperoxide resistance regulator, OhrR; QM/MM, quantum mechanical/molecular mechanical; NBO, natural bond orbital; PES, potential energy surface

REFERENCES

(1) Feldhammer, M.; Uetani, N.; Miranda-Saavedra, D.; Tremblay, M. L. *Crit. Rev. Biochem. Mol. Biol.* **2013**, *48*, 430−445.

(2) Tonks, N. K. *Nat. Rev. Mol. Cell Biol.* **2006**, *7*, 833−846.

(3) Yip, S. C.; Saha, S.; Chernoff, J. *Trends Biochem. Sci.* **2010**, *35*, 442−449.

(4) Tonks, N. K. *Febs J.* **2013**, *280*, 346−378.

(5) Bence, K. K.; Delibegovic, M.; Xue, B.; Gorgun, C. Z.; Hotamisligil, G. S.; Neel, B. G.; Kahn, B. B. *Nat. Med.* **2006**, *12*, 917−924.

(6) Gonzalez-Rodriguez, A.; Gutierrez, J. A. M.; Sanz-Gonzalez, S.; Ros, M.; Burks, D. J.; Valverde, A. M. *Diabetes* **2010**, *59*, 588−599.

(7) Ali, M. I.; Ketsawatsomkron, P.; de Chantemele, E. J. B.; Mintz, J. D.; Muta, K.; Salet, C.; Black, S. M.; Tremblay, M. L.; Fulton, D. J.; Marrero, M. B.; Stepp, D. W. *Circ. Res.* **2009**, *105*, 1013−1022.

(8) Chatelain, E. H.; Dupuy, J. W.; Letellier, T.; Dachary-Prigent, J. *Cell. Mol. Life Sci.* **2011**, *68*, 2603−2613.

(9) Zhu, S.; Bjorge, J. D.; Fujita, D. J. *Cancer Res.* **2007**, *67*, 10129−10137.

(10) Dube, N.; Cheng, A.; Tremblay, M. L. *Proc. Natl. Acad. Sci. U. S. A.* **2004**, *101*, 1834−1839.

(11) Combs, A. P. *J. Med. Chem.* **2010**, *53*, 2333−2344.

(12) Lessard, L.; Stuible, M.; Tremblay, M. L. *BBA-Proteins Proteomics* **2010**, *1804*, 613−619.

(13) Sobhia, M. E.; Paul, S.; Shinde, R.; Potluri, M.; Gundam, V.; Kaur, A.; Haokip, T. *Expert Opin. Ther. Patents* **2012**, *22*, 125−153.

(14) Brandao, T. A. S.; Hengge, A. C.; Johnson, S. J. *J. Biol. Chem.* **2010**, *285*, 15874−15883.

(15) Salmeen, A.; Andersen, J. N.; Myers, M. P.; Meng, T. C.; Hinks, J. A.; Tonks, N. K.; Barford, D. *Nature* **2003**, *423*, 769−773.

(16) Parsons, Z. D.; Gates, K. S. *Biochemistry* **2013**, *52*, 6412−6423.

(17) van Montfort, R. L. M.; Congreve, M.; Tisi, D.; Carr, R.; Jhoti, H. *Nature* **2003**, *423*, 773−777.

(18) Sivaramakrishnan, S.; Cummings, A. H.; Gates, K. S. *Bioorg. Med. Chem. Lett.* **2010**, *20*, 444−447.

(19) Shetty, V.; Neubert, T. A. *J. Am. Soc. Mass Spectrom.* **2009**, *20*, 1540−1548.

(20) Yang, J.; Groen, A.; Lemeer, S.; Jans, A.; Slijper, M.; Roe, S. M.; den Hertog, J.; Barford, D. *Biochemistry* **2007**, *46*, 709−719.

(21) Lee, J. W.; Soonsanga, S.; Helmann, J. D. *Proc. Natl. Acad. Sci. U. S. A.* **2007**, *104*, 8743−8748.

(22) Dokainish, H. M.; Gauld, J. W. *Biochemistry* **2013**, *52*, 1814−1827.

(23) Nakamura, T.; Yamamoto, T.; Abe, M.; Matsumura, H.; Hagihara, Y.; Goto, T.; Yamaguchi, T.; Inoue, T. *Proc. Natl. Acad. Sci. U. S. A.* **2008**, *105*, 6238−6242.

(24) Zhang, Z. Y.; Dixon, J. E. *Biochemistry* **1993**, *32*, 9340−9345.

(25) Haque, A.; Andersen, J. N.; Salmeen, A.; Barford, D.; Tonks, N. K. *Cell* **2011**, *147*, 185−198.

(26) Sarma, B. K.; Mugesh, G. *J. Am. Chem. Soc.* **2007**, *129*, 8872−8881.

(27) Sarma, B. K. *J. Mol. Struct.* **2013**, *1048*, 410−419.

(28) Zeida, A.; Guardia, C.; Lichtig, P.; Perissinotti, L.; Defelipe, L.; Turjanski, A.; Radi, R.; Trujillo, M.; Estrin, D. *Biophys Rev.* **2014**, 1−20.

(29) Molecular Operating Environment (MOE); Chemical Computing Group Inc: Montreal, Quebec, Canada, 2012.

(30) Phillips, J. C.; Braun, R.; Wang, W.; Gumbart, J.; Tajkhorshid, E.; Villa, E.; Chipot, C.; Skeel, R. D.; Kale, L.; Schulten, K. *J. Comput. Chem.* **2005**, *26*, 1781−1802.

(31) Labute, P. *Proteins* **2009**, *75*, 187−205.

(32) Cornell, W. D.; Cieplak, P.; Bayly, C. I.; Gould, I. R.; Merz, K. M.; Ferguson, D. M.; Spellmeyer, D. C.; Fox, T.; Caldwell, J. W.; Kollman, P. A. *J. Am. Chem. Soc.* **1996**, *118*, 2309−2309.

(33) Salomon-Ferrer, R.; Case, D. A.; Walker, R. C. *Wiley Interdiscip. Rev.-Comput. Mol. Sci.* **2013**, *3*, 198−210.

(34) Gerber, P. R.; Muller, K. J. *Comput.-Aided Mol. Des.* **1995**, *9*, 251−268.

(35) Frisch, M. J.; Trucks, G. W.; Schlegel, H. B.; Scuseria, G. E.; Robb, M. A.; Cheeseman, J. R.; Scalmani, G.; Barone, V.; Mennucci, B.; Petersson, G. A.; Nakatsuji, H.; Caricato, M.; Li, X.; Hratchian, H. P.; Izmaylov, A. F.; Bloino, J.; Zheng, G.; Sonnenberg, J. L.; Hada, M.; Ehara, M.; Toyota, K.; Fukuda, R.; Hasegawa, J.; Ishida, M.; Nakajima, T.; Honda, Y.; Kitao, O.; Nakai, H.; Vreven, T.; Montgomery, J. A., Jr.; Peralta, J. E.; Ogliaro, F.; Bearpark, M.; Heyd, J. J.; Brothers, E.; Kudin, K. N.; Staroverov, V. N.; Kobayashi, R.; Normand, J.; Raghavachari, K.; Rendell, A.; Burant, J. C.; Iyengar, S. S.; Tomasi, J.; Cossi, M.; Rega, N.; Millam, J. M.; Klene, M.; Knox, J. E.; Cross, J. B.; Bakken, V.; Adamo, C.; Jaramillo, J.; Gomperts, R.; Stratmann, R. E.; Yazyev, O.; Austin, A. J.; Cammi, R.; Pomelli, C.; Ochterski, J. W.; Martin, R. L.; Morokuma, K.; Zakrzewski, V. G.; Voth, G. A.; Salvador, P.; Dannenberg, J. J.; Dapprich, S.; Daniels, A. D.; Farkas, O.; Foresman, J. B.; Ortiz, J. V.; Cioslowski, J.; Fox, D. J. *Gaussian 09*; Gaussian, Inc.: Wallingford, CT, 2009.

(36) Zhao, Y.; Truhlar, D. G. *Theor. Chem. Acc.* **2008**, *120*, 215−241.

(37) Simard, D.; Dokainish. H. M., Gauld, J. W.; manuscript in preparation.

(38) Gomez, H.; Polyak, I.; Thiel, W.; Lluch, J. M.; Masgrau, L. *J. Am. Chem. Soc.* **2012**, *134*, 4743−4752.

(39) Polyak, I.; Reetz, M. T.; Thiel, W. *J. Phys. Chem. B* **2013**, *117*, 4993−5001.

(40) Biegler-König, F.; Schönbohm, J. *AIM2000*, version 2.0; University of Applied Science: Bielefeld, Germany, 2002.

(41) (a) Lonsdale, R.; Ranaghan, K. E.; Mulholland, A. J. *Chem. Commun.* **2010**, *46*, 2354−2372. (b) de Visser, S. P.; Quesne, M. G.; Martin, B.; Comba, P.; Ryde, U. *Chem. Commun.* **2014**, *50*, 262−282. (c) Senn, H. M.; Thiel, W. *Angew. Chem., Int. Ed. Engl.* **2009**, *48*, 1198−1229. (d) Shaik, S.; de Visser, S. P.; Kumar, D.; Altun, A.; Thiel, W. *Chem. Rev.* **2005**, *105*, 2279−2328.

(42) van der Kamp, M. W.; Mulholland, A. J. *Biochemistry* **2013**, *52*, 2708−2728.

(43) Lonsdale, R.; Houghton, K. T.; Zurek, J.; Bathelt, C. M.; Foloppe, N.; de Groot, M. J.; Harvey, J. N.; Mulholland, A. J. *J. Am. Chem. Soc.* **2013**, *135*, 8001−8015.

(44) Ribeiro, A. J. M.; Ramos, M. J.; Fernandes, P. A. *J. Am. Chem. Soc.* **2012**, *134*, 13436−13447.

DOI: 10.1021/cs501707h
ACS Catal. 2015, 5, 2195−2202

(45) Takahashi, O.; Oda, A. Amide−iminol tautomerization of the C-terminal peptide groups of aspartic acid residues: Two-water-assisted mechanism, cyclization from the iminol tautomer leading to the tetrahedral intermediate of succinimide formation, and implication to peptide group hydrogen exchange. In *Tyrosine and Aspartic Acid: Properties, Sources and Health Benefits*, Jones, J. E., Morano, M., Eds.; Nova Science Publishers: New York, 2012; pp 131−147.
(46) Takahashi, O. *Health* **2013**, *5*, 2018−2021.
(47) Iwaoka, M.; Isozumi, N. *Molecules* **2012**, *17*, 7266−7283.
(48) Nakanishi, W.; Hayashi, S.; Narahara, K. *J. Phys. Chem. A* **2008**, *112*, 13593−13599.
(49) Adhikari, U.; Scheiner, S. *Chem. Phys. Lett.* **2011**, *514*, 36−39.
(50) Scheiner, S. *J. Chem. Phys.* **2011**, *134*, 1−9.

DOI: 10.1021/cs501707h
ACS Catal. 2015, 5, 2195−2202